CaM Kinase II-δ is required for diabetic hyperglycemia and retinopathy but not nephropathy

Jessy Chen[1,2], Thomas Fleming[3], Sylvia Katz[1,2], Matthias Dewenter[1,2], Kai Hofmann[1,2], Alireza Saadatmand[1,2], Mariya Kronlage[1,2,4], Moritz P. Werner[1,2], Bianca Pokrandt[5], Friederike Schreiter[1,2], Jihong Lin[6], Daniel Katz[1,2], Jakob Morgenstern[3], Ahmed Elwakiel[7], Peter Sinn[8], Hermann-Josef Gröne[9,10], Hans-Peter Hammes[6], Peter P. Nawroth[3,11,12], Berend Isermann[7], Carsten Sticht[13], Britta Brügger[5], Hugo A. Katus[2,4], Marco Hagenmueller[1,2,*] and Johannes Backs[1,2,*]

[1] Institute of Experimental Cardiology, Heidelberg University, Heidelberg, Germany
[2]German Center for Cardiovascular Research (partner site Heidelberg/Mannheim), Heidelberg, Germany
[3] Department of Internal Medicine I and Clinical Chemistry, University Hospital of Heidelberg, Heidelberg, Germany.
[4] Department of Cardiology, University of Heidelberg, Heidelberg, Germany
[5]Heidelberg University Biochemistry Center, INF 328, 69120 Heidelberg, Germany.
[6] 5th Medical Department, Medical Faculty Mannheim, University of Heidelberg, D-68169, Mannheim, Germany
[7]Institute of laboratory medicine, clinical chemistry, and molecular diagnostics (ILM), University of Leipzig, Leipzig, Germany Department of Pathology, Heidelberg University Hospital, Heidelberg, Germany
[9] Department of Cellular and Molecular Pathology, German Cancer Research Center, Heidelberg, Germany
[10] Institute of Pathology, University of Marburg, Marburg, Germany.
[11] German Center for Diabetes Research (DZD), Neuherberg, Germany.
[12] Institute for Diabetes and Cancer IDC Helmholtz Center Munich, Germany & Joint Heidelberg-IDC Translational Diabetes Program, Neuherberg, Germany.
[13]Medical Research Center, Medical Faculty Mannheim, Heidelberg University, Mannheim, Germany

* these authors contributed equally

Running title: CaMKIIδ regulates diabetic hyperglycemia
Word count: 3920 (main text)

Corresponding author:
Johannes Backs
mail: johannes.backs@med.uni-heidelberg.de
Phone: +49-6221-5637714

Diabetes Publish Ahead of Print, published online November 25, 2020

Abstract

Type 2 diabetes has become a pandemic and leads to late diabetic complications of organs including kidney and eye. Lowering hyperglycemia is the typical therapeutic goal in clinical medicine. However, hyperglycemia may only be a symptom of diabetes but not the sole cause of late diabetic complications, Instead, other diabetes-related alterations could be causative. Here, we studied the role of CaM Kinase II δ (CaMKIIδ) that is known to be activated through diabetic metabolism. CaMKIIδ is expressed ubiquitously and might therefore affect several different organ systems. We crossed diabetic leptin receptor mutant mice to mice lacking CaMKIIδ globally. Remarkably, CaMKIIδ-deficient diabetic mice did not develop hyperglycemia. As potential underlying mechanisms, we provide evidence for improved insulin sensing with increased glucose transport into skeletal muscle but also reduced hepatic glucose production. Despite normoglycemia, CaMKIIδ-deficient diabetic mice developed the full picture of diabetic nephropathy but diabetic retinopathy was prevented. We also unmasked a retina-specific gene expression signature that might contribute to CaMKII-dependent retinal diabetic complications. These data challenge the clinical concept of normalizing hyperglycemia in diabetes as a causative treatment strategy for late diabetic complications and call for a more detailed analysis of intracellular metabolic signals in different diabetic organs.

Introduction

Since 1980 the global prevalence of Type 2 Diabetes (T2D) has doubled. In 2014, over 420 million people were suffering from T2D (1). Late diabetic complications in organs like kidney and eye can lead to kidney failure and blindness. Hyperglycemia has long been suggested to cause diabetic late complications (2). Based on this assumption, numerous therapeutic strategies were developed to reduce blood glucose levels. However, some patients with well-adjusted glycemic control still develop late diabetic complications whereas others with less adequate control do not (3). Thus, it must be debated whether hyperglycemia is only a symptom of diabetes whereas other diabetes-related metabolic signaling cause late diabetic complications.
Here, we focused on CaM Kinase II (CaMKII) that has been shown to be activated in diabetes (4). CaMKII is a serine/threonine protein kinase with a broad spectrum of substrates, consisting of four isoforms. The α- and β-isoforms are almost exclusively expressed in the brain whereas the δ- and γ isoforms are ubiquitously expressed with higher expression levels of CaMKIIδ in most organs (5). Besides $Ca^{2+/}$Calmodulin-binding, diabetes-related post-translational modifications including oxidation and O-GlcNAcylation lead to CaMKII activation (6-8). CaMKII in turn is known to regulate hepatic glucose production (HGP) thereby potentially elevating plasma glucose levels (9-11). However, the role of CaMKII for late diabetic complications is unclear.
We crossed leptin receptor mutant mice ($Lepr^{db/db}$) as a model of T2D to mice with a global CaMKIIδ deletion (KO). We show for the first time that CaMKIIδ plays a crucial role in regulating diabetic hyperglycemia. To our great surprise, CaMKIIδ was required for diabetic hyperglycemia and retinopathy but not nephropathy.

Materials and Methods

Generation of CaMKIIδ-deficient Lepr$^{db/db}$ mice. CaMKIIδ-deficient (KO) (12) were crossed to Lepr$^{db/db}$ mice (Jackson lab) to obtain CaMKIIδ-deficient Lepr$^{db/db}$ (Lepr$^{db/db}$/KO) and Lepr$^{+/+}$ (Lepr$^{+/+}$/KO) as compared to Lepr$^{db/db}$/WT and Lepr$^{+/+}$/KO. These mice were maintained in a C57BL/6J genetic background, received a standard diet and kept on a 12h light and dark cycle at 22 ± 2°C and room humidity of 55%. All experimental procedures were reviewed and approved by the Institutional Animal Care and Use Committee at the Regierungspräsidium Karlsruhe, Germany.

Measurement of blood glucose and glycated haemogloblin (HbA1c). Blood glucose was measured with Accu-Check Aviva III (Roche). HbA1c was determined by cation-exchange chromatography on a PolyCAT A column (PolyLC Inc.). The relative amount of HbA1c is expressed as a percentage of Hb, based upon the area under the respective peaks.

Glucose Tolerance Test (GTT) and Insulin Tolerance Test (ITT). 12-16 weeks old mice were starved for 12 or 4 hours, respectively, then glucose (2g/g body-weight solved in 0.9% NaCl) or insulin (0.0005U/g body-weight solved in 0.9% NaCl) were injected intraperitoneally (ip). Blood glucose was measured from tail vain blood at baseline and at the timepoints 15min, 30min, 60min and 120min after ip-injection.

Quantification of vasoregression and pericyte loss in retinae. Acellular capillaries and pericyte loss were evaluated in retinal digest preparations as described previously (13). For visualization of the retinal morphology and morphometry, PAS staining was performed on digested retinae. Quantification of acellular capillaries was done using the Cell^{F} software (Olympus Opticals, Hamburg, Germany). The number of acellular capillaries was calculated to the total retinal area. The number of pericytes was quantified in the ten randomly selected fields in the central retina under 400x magnification by a blinded observer.

Quantification of mesangial expansion in kidney. Kidneys were fixed in 4% formalin and embedded in paraffin. Periodic acid- Schiff (PAS) staining was performed on kidney paraffin sections. PAS stainings were scanned at 40x magnification using the Aperio AT2 Digital Pathology Slide Scanner (Leica) for digital microscopy. The mean mesangial expansion was quantified blinded in 60 randomly selected glomeruli per kidney with ImageJ software.

Basal membrane thickness. The method of estimating the thickening of the basal membrane was described previously (14). In brief, specimen are fixed with Karnovsky and dehydrated with an alcohol series and embedded in araldite (SERVA). Sections of 70nm thickness were cut using an Ultracut E microtome (Leica, Wetzlar, Germany). Sections were analyzed with a ZEISS EM 900 or 910 transmission-electron microscope (ZEISS, Oberkochen; Germany) and macrographs are taken with a CCDK2 camera (TRS-Tröndle, Dünzelbach; Germany). Basal membrane thickness was estimated with the ImageSP software (TRS-Tröndle).

Quantification of Proteinuria. Proteinuria was measured with collected spot urine using the Mouse Albumin Elisa Quantification Kit (Bethyl Laboratories, E90-134). In brief, a 96-well-plate was coated (1h), washed (5x) and blocked (30min) with corresponding antibody and solutions. Diluted urine samples and a prepared standard were added in duplicates and incubated for 1 hour. Subsequently, the plate was washed again and the HRP detection antibody was added to each well and incubated for another hour. Afterwards, the plate was developed protected from light for 15min with TMB substrate solution and the reaction was stopped with stopping dilution. The absorbance was measured in a micro-plate reader at 450nm (EnSpire, Multi-Mode reader, Perkin Elmer).

WT-1 immunohistochemistry. Paraffin kidney sections were dewaxed, rehydrated then incubated with citrate-based antigen retrieval solution (H-3300, Vector laboratories). Endogenous peroxidase activity was blocked by incubating the sections with 3% hydrogen peroxide solution. Sections were then blocked with PBS containing 3% donkey serum and 0.5% Triton X-100 for one hour at room temperature. Sections

were incubated with primary antibody against WT-1 (ab89901, Abcam) in a dilution of 1:300 overnight at 4 °C. Rest of the staining protocol and analysis was performed as previously described (15).

Masson's Trichrome staining (MTS). Paraffin kidney sections were dewaxed, rehydrated then stained using the trichrome staining kit (HT15, Sigma) according to the manufacturer's instructions. The slides were then dehydrated and mounted using anhydrous mounting medium (6638.1, Carl Roth). Ten visual fields per mouse kidney were randomly selected and the percent of fibrotic area was determined using ImageJ software.

Western Blotting. Proteins were isolated from homogenized tissue or from transfected M1 and MES13 cells with RIPA buffer. Protein concentrations were determined with BCA. Western Blot analysis was performed with 10% SDS-gels and proteins were blotted on nitrocellulose membranes. Membranes were blocked with 5% skim milk or 5%BSA, incubated with primary antibodies overnight and secondary antibodies for 1h on the next day. Detection was performed with Luminol Reagent (Santa Cruz). Antibodies used for immunoblotting were anti-GLUT1 (abcam, 1:1000), anti-GLUT4 (LS Bio, 1:1000 or Santa Cruz 1:1000), anti-CaMKII (BD Bioscience, 1:1000), anti-Tubulin (Sigma, 1:2000), anti-GAPDH (Chemicon, 1:10000), anti-p38MAPK (Cell Signaling, 1:1000), anti-p-p38MAPK (Cell Signaling, 1:1000) and β-actin (1:2000; Cell Signaling, 4967S; rabbit).

Quantitative real-time PCR. RNA was isolated using TRIzol (TRI Reagent, Sigma). cDNA synthesis was carried out with First Strand cDNA Synthesis Kit (Thermo Fisher Scientific). qPCR was performed with the Universal Probe Library System (Roche) using the TaqMan Universal PCR Mastermix (Applied Biosystems) and detection on a 7500 fast cycler (Applied Biosystems). Primers and probes used were 5'-aacccgttttctgggttga-3' and atgtgtgggcgatgacatt (Probe #105) for Pck-1, 5'-gaaagtttcagccacagcaa-3' and tctgtcccggatctaccttg (Probe #19) for G6pc and 5'-acaccatgctccgtcctg-3' and 5'-gtcattggtgttggcttgtg-3' (Probe #98) for SGLT2, 5'-cctggccatagaggtgga-3' and ggggagaggtatccaggtgt (#32) for CaMK2a, 5'-

agccccaaaggatctctcc-3’ and gggttatggataacggtggtt (#74) for CaMK2b, 5’-gatcaaagctggagcctacg-3’ and gcttcaggagtgactgtgtcc (#9) for CaMK2g, 5’-agttcacagggacctgaagc-3’ and cgccttgaacttctatggcta (#68) for CaMK2d, 5’-ctggcaggccgaagtatg-3’ and ttccaatgttactggcaaagag (#49) for SGLT1. Relative changes in gene expression measured with real-time quantitative PCR were analyzed using the 2(-Delta Delta C(T)) method (16).

Cell culture. Murine kidney epithelial (M1) and mesangial (MES13) cells, immortalized with SV40 large T antigen were obtained from ATCC® (Mannassas, Virginia). A mixture of four siRNAs targeting murine CaMKIIδ were purchased from Horizon Discovery Ltd (siGENOME, M-040821-01). 1 x 10^6 cells were transfected with a total of 500pmol siRNA in 100µl resuspension buffer by electroporation using the Neon transfection system (Thermo, Karlsruhe, Germany). Cells were also transfected with a non-targeting pool (siGENOME, D-001206-14) as a negative control.

Glycogen and sorbitol . Glycogen and sorbitol content of muscle tissue(s) were measured end-point, colorimetric assay (Biovision) according to manufacturer instructions and normalized to total protein content, as determined by the Bradford assay.

Plasma Insulin. Plasma insulin was measured by sandwich immunoassay (ALPCO), according to manufacturer instructions.

MG levels. MG levels were determined by liquid chromatography followed by tandem mass spectrometric detection (LC-MS/MS), as described previously (17).

RNA Sequencing and Analysis. Most of the procedure was done with R and bioconductor using the NGS analysis plackage systempipeR (18). Quality control of raw sequencing reads was performed using FastQC (Babraham Bioinformatics). Low-quality reads were removed using trim_galore (version 0.6.4). The resulting reads were aligned to mouse genome version GRCm38.p6 from Genecode and counted using kallisto version 0.46.1 (19). The count data. was transformed to log2-

counts per million (logCPM) using the voom-function from the limma package (20). Differential expression analysis was performed using the limma package in R. A false positive rate of α= 0.05 with FDR correction was taken as the level of significance. Volcano plots and heatmaps were created using ggplot2 package (version 2.2.1) and the complexHeatmap (version 2.0.0) (21). Pathway analysis was made with fgsea package (22) and the enrichmentbrowser package (23) in R using the pathway information from KEGG database (https://www.genome.jp/kegg/pathway.html).

Lipidomics. Samples (approx. 2 -4 nmol of total lipid) were subjected to an acidic Bligh and Dyer liquid-liquid extraction (24) . Lipid standards were added prior to extractions, using a master mix as described (25). Samples were analyzed on an QTRAP 6500+ mass spectrometer (Sciex) with chip-based (HD-D ESI Chip, Advion Biosciences) electrospray infusion and ionization via a Triversa Nanomate (Advion Biosciences) as described (26). Data evaluation was done using LipidView (1.3 beta, Sciex) and an in-house-developed software (ShinyLipids).

Statistical analysis. Results are expressed as the mean ± SD. Statistical analysis was performed with GraphPad Prism (Version 6.0, GraphPad Software Inc., CA, USA). Statistical analyses were performed using 1-way ANOVA where appropriate. $p < 0.05$ was considered statistically significant.

Results

CaMKIIδ-deficient Lepr$^{db/db}$ mice are hyperinsulinemic but not hyperglycemic. Lepr$^{db/db}$/KO were viable and had comparable body-weights as Lepr$^{db/db}$/WT littermates **(Suppl. Fig. 1)**. Apart from mildly elevated glucose levels at early age, Lepr$^{db/db}$/KO did not develop hyperglycemia at age >16 weeks as compared to Lepr$^{db/db}$/WT **(Fig.1A/B)**. Likewise, HbA1c levels in Lepr$^{db/db}$/KO were equal to WT and KO **(Fig. 1C)**. Insulin plasma levels were equally elevated in Lepr$^{db/db}$/KO as in Lepr$^{db/db}$/WT **(Fig. 1D)**.

CaMKIIδ deficiency improves insulin responsiveness. We next conducted GTT and ITT. Glucose tolerance was impaired in both Lepr$^{db/db}$/WT and Lepr$^{db/db}$/KO with prolonged hyperglycemia **(Fig. 2A)**. Upon insulin injection, blood glucose levels of Lepr$^{db/db}$ paradoxically increased , which we attribute to an endogenous stress response and/or dysregulated insulin sensing. Notably, this effect was reduced in Lepr$^{db/db}$/KO as compared to Lepr$^{db/db}$/WT, indicating that CaMKIIδ mutation restores whole body insulin responsiveness but not glucose tolerance in leptin mutant mice **(Fig. 2B)**.

Evidence for increased glucose transport into skeletal muscle and for downregulated hepatic glucose production in CaMKIIδ-deficient Lepr$^{db/db}$ mice. In skeletal muscle – a major glucose store of the body – protein levels of the insulin-independent glucose transporter GLUT1 and the insulin-dependent glucose transporter GLUT4 (27) were increased in both Lepr$^{db/db}$/WT and Lepr$^{db/db}$/KO **(Fig. 3A-B)**. However, GLUT1 and GLUT4 were also up-regulated in non-diabetic KO, pointing to a general CaMKIIδ-dependent mode of GLUT expression. The additional increase in expression of the insulin-dependent transporter GLUT4 in skeletal muscle of Lepr$^{db/db}$/KO is suggestive to contribute to the prevention of hyperglycemia. In support, skeletal muscle glycogen content was relatively higher increased in Lepr$^{db/db}$/KO **(Fig. 3C)**. The glucose intermediate sorbitol of the polyol pathway was not significantly enhanced in Lepr$^{db/db}$ mice but we observed a trend towards elevation in Lepr$^{db/db}$/KO **(Suppl Fig. 2)**.

Hepatic glycogen content was not significantly decreased **(Suppl. Fig. 3A)** while sorbitol levels were increased in both Lepr$^{db/db}$ groups **(Suppl. Fig. 3B)**, indicating

that glucose enters the polyol pathway, which might result in higher oxidative stress and the formation of AGEs.

To investigate whether CaMKIIδ regulates HGP, we examined the levels of phosphorylated p38 MAPK, which regulates the localization of the transcriptional regulator of hepatic glucose production FoxO1 (28), and found it to be attenuated in Lepr$^{db/db}$/KO **(Suppl. Fig. 4A-B)**. Moreover, gene expression of phosphoenolpyruvate carboxykinase (Pck-1) and glucose-6-phosphatase (G6pc) - two key enzymes of gluconeogenesis - are downregulated in CaMKIIδ-deficient db/db mice (**Suppl. Fig. 4C-D)**, pointing to a contribution of CaMKIIδ to the activation of hepatic glucose production. In the liver of in Lepr$^{db/db}$/WT, we did not observe an upregulation of CaMKIγ which was implied to regulate HGP, pointing to a specific yet unknown effect of CaMKIIδ on HGP (**Suppl. Fig. 4E**).

Whereas mRNA levels of the sodium/glucose-cotransporter 2 (SGLT2) were slightly but not significantly increased in kidneys of Lepr$^{db/db}$/KO, SGLT1 mRNA was increased in Lepr$^{db/db}$/WT but not in Lepr$^{db/db}$/KO **(Suppl. Fig. 5A-B).** But, as urinary glucose concentrations were decreased in Lepr$^{db/db}$/KO as compared to Lepr$^{db/db}$/WT littermates **(Suppl. Fig. 5C),** it seems rather unlikely that a decrease in renal glucose excretion contributes to low blood glucose levels**.**

More studies are needed to determine the relative contributions of the observed changes to the here described phenoptye.

Diabetic nephropathy despite normoglycemia in CaMKIIδ-deficient Lepr$^{db/db}$ mice. To our big surprise, we observed more pronounced mesangial expansion in Lepr$^{db/db}$/KO despite normoglycemia as compared to hyperglycemic Lepr$^{db/db}$/WT kidneys **(Fig. 4A)**. Likewise, thickening of the basal membrane **(Fig. 4B)** and loss of podocytes **(Fig. 4C)** were more pronounced. Furthermore, we observed fibrosis **(Fig.4D)**, tubular dilatation **(Fig. 4E)** and proteinuria **(Fig. 4F)** in Lepr$^{db/db}$/KO as in Lepr$^{db/db}$/WT. Kidney weight was slightly elevated in 16 week old Lepr$^{db/db}$/KO and glomerulum size increased over time in both Lepr$^{db/db}$ groups (**Suppl. Fig. 6A-D**). These data show that diabetic nephropathy in Lepr$^{db/db}$ can even occur under normoglycemia. This is a central finding of this study, highlighting that the development of diabetic nephropathy is a complex process that is not determined by glucose levels in the blood.

Because CaMKIIα and CaMKIIβ were undetectable and CaMKIIγ was not increased in Lepr$^{db/db}$/KO, it is unlikely that other isoforms compensated to induce nephropathy (**Suppl. Fig. 7A**). Indeed, phosphorylated calcineurin, a marker for CaMKII activity (29), was increased in renal tissue of Lepr$^{db/db}$/WT but not Lepr$^{db/db}$/KO (**Fig. 4G**), confirming that CaMKIIδ contributed entirely to elevated CaMKII activity in diabetic kidneys.

Evidence for increased renal glucose uptake in normoglycemic CaMKIIδ-deficient Lepr$^{db/db}$ mice. GLUT1 expression was elevated in Lepr$^{db/db}$/WT but also in Lepr$^{+/+}$/KO **(Fig. 5A)** and GLUT4 was slightly but not significantly increased in both KO groups**,** suggestive for increased renal glucose uptake in KO. In Seahorse experiments, siRNA-mediated CaMKIIδ deletion in immortalised tubular cells (M1) and mesangial cells (MES13) did not reveal differences in the glycolysis stress tests, suggesting that substrate utilization for energy production in mesangial and tubular cells is not regulated by CaMKIIδ **(Suppl. Fig. 8A-D)**. Therefore, we speculated that the higher glucose uptake in Lepr$^{db/db}$/KO does not contribute to energy production via glycolysis but 'fuels' glycolysis side pathways, that may result in accumulation of reactive glucose metabolites. Thus, we measured total O-GlcNAcylation in renal tissue (30), and we found elevated protein O-GlcNAcylation in Lepr$^{db/db}$/WT and Lepr$^{db/db}$/KO but also in Lepr$^{+/+}$/KO **(Fig. 5B),** suggesting that protein O-GlcNAcylation is governed by CaMKIIδ. Methylglyoxal (MG) has been suggested as another diabetes-associated reactive glucose metabolite (31). We measured levels of MG in the kidney and found increased concentrations in both Lepr$^{db/db}$/WT and Lepr$^{db/db}$/KO mice compared to their respective non-diabetic littermates **(Fig. 5C),** suggesting that MG is CaMKIIδ-independently produced and may be additive to renal protein O-GlcNAcylation as cause for diabetic nephropathy.

No diabetic retinopathy in normoglycemic CaMKIIδ-deficient Lepr$^{db/db}$ mice. As markers for diabetic retinopathy we measured the number of acellular capillaries, pericytes and migrating pericytes (32) **(Fig. 6A)**. Lepr$^{db/db}$/WT showed a significant increase in the number of acellular capillaries **(Fig. 6B)**, a loss of pericytes **(Fig. 6C)** and a higher number of migrating pericytes **(Fig. 6D)** compared to non-diabetic mice. Remarkably, Lepr$^{db/db}$/KO did not show pathological alterations in the aforementioned parameters, indicating that these mice are protected from diabetic retinopathy. Other

than in kidney, we found a general upregulation of all CaMKII genes in Lepr$^{db/db}$/WT but surprisingly not in Lepr$^{db/db}$/KO (**Suppl. Fig. 7B**), pointing to a yet known positive feedback loop of CaMKIIδ- or diabetes-induced CaMKIIα –, CaMKIIβ –, CaMKIIγ – gene expression. The profound changes in CaMKII gene expression prompted us to systematically analyze diabetes-related gene expression in different diabetic organs by RNAseq (GSE157739 provides access to all data). In analogy to the clear CaMKIIδ-dependent phenotypic data, we found a clear pattern of CaMKII-dependent differential gene expression in the retina as compared to the kidney (**Suppl. Fig. 9A-B**). We were particularly interested in the genes that were only regulated in WT retina under diabetic conditions but not in KO (CaMKII-dependent specific diabetic retinopathy genes; **Fig. 6E-F**) and in genes that were regulated in WT retina and kidney under diabetic conditions but not in KO retina (**Fig. 6E, Suppl. Fig. 9C-D**). A few of the top-regulated genes in the retina (**Suppl. Fig. 9A-B**) were retina-specific (**marked in red, Fig. 6C**). The signature of retina-specific and CaMKIIδ-dependent diabetes-induced genes need further functional analysis. Many genes, e.g. Gpat2, with “lipid” as keyword in Gene Ontology were differentially regulated in the retina of Lepr$^{db/db}$/WT vs Lepr$^{+/+}$/WT but not Lepr$^{db/db}$/KO vs Lepr$^{+/+}$/KO (**Suppl. Fig. 10A**) whereas CaMKIIδ-dependent changes in the kidney was less clear (**Suppl. Fig. 10B).** In an attempt to validate the significance of retinal gene expression changes concerning lipid mediators, we failed to identify differences by lipidomics (**Suppl. Fig. 10C)**. Specific diabetes-induced phosphatidylethanolamine (PE) and Cholesterol (Chol) reduction in the retina appeared to be CaMKIIδ-dependent (**Suppl. Fig. 10D-F**) but the detectable quantitative differences questionably contribute to the striking phenotype rescue **(Suppl. Fig. 10G)**.

Discussion

In this study we show 1) that CaMKIIδ induces diabetic hyperglycemia possibly by reducing insulin sensing with decreased glucose uptake into stores and an increase in HGP, 2) that hyperglycemia per se does not lead to diabetic nephropathy and 3) that hyperglycemia is a good measure to assess the risk of diabetic retinopathy.

To date, little is known about the role of CaMKII in insulin signalling and the regulation of GLUTs. In a rat skeletal muscle cell line, CaMKII mediates phosphorylation of the insulin receptor substrate 1 (IRS1) at Serine 612 and this in turn blocks downstream signalling of the insulin receptor (33). As a consequence, expression of GLUT4 is inhibited, indicating that CaMKII regulates GLUT4 expression via the insulin signalling pathway in their model system. Another report describes the regulation of GLUT4 through CaMKII on gene expression level via the transcription factor myocyte enhancer factor 2 (MEF2) (34) - a prominent downstream target of CaMKII signalling (35).

Regarding the influence of CaMKIIδ on HGP, it has been shown that CaMKIIγ is a regulator of HGP (9-11; 36). Compared to the aforementioned study we observed a similar but more modest impact of CaMKIIδ on HGP. However, the seemingly lower impact of CaMKIIδ deficiency on baseline glucose production in the liver is may be due to a compensatory activation of CaMKIIγ and suggest that CaMKIIγ is the more predominant isoform involved in hepatic glucose production. However, in the liver CaMKIIγ is not upregulated in a CaMKIIδ-dependent manner as in the diabetic retina, suggesting that either CaMKIIδ contributes to HGP in the diabetic liver more than CaMKIIγ or that CaMKIIγ compensates at the functional levels as it was described in pathological cardiac remodelling (29).

Another striking finding is that the CaMKIIδ-dependent reduction of blood glucose in $Lepr^{db/db}$/KO mice does not affect the integrity of all organ systems to the same extent (i.e., no effect on diabetic nephropathy but on retinopathy), indicating that diabetes-related defects occur in a tissue and cell-type specific manner. This observation challenges the prevailing idea that reducing hyperglycemia is a unifying target to limit late complications in diabetic patients. We propose, that not the clinical presentation of hyperglycemia but rather specific not well-defined alterations of glucose handling and the production of glucose metabolites such as MG or O-GlcNAc contribute more directly to late diabetic complications.

Accordingly, the opposite phenotypes observed in the kidney and the retinae of $Lepr^{db/db}$/KO mice can be explained by specific differences in glucose metabolism in these organs. A recent study described tissue-specific alterations in kidney and

retinae in diabetic vs. non-diabetic mice using transcriptomics, metabolomics and metabolic flux analyses (37). However, whereas in this study the activity of glucose and fatty acid metabolism was more enhanced in the kidney than the retina, we found more specific gene expression signatures in the retina, which depended largely on CaMKII. However, we closely checked the possible contribution of lipid metabolites but could not provide evidence for a significant contribution. While renal glucose metabolites such as MG and O-GlcNAc persisted in CaMKIIδ-deficient mice, the retina showed e.g. a significant attenuation of the rate limiting enzyme of the hexosamine biosynthesis pathway in a CaMKII-dependent manner.

Based on the collected data, we cannot distinguish whether the observed retinoprotection depends directly on normoglycemia or retinal CaMKIIδ itself. The latter is supported by an *in vitro* study with primary cultures of retinal Müller cells prepared from Sprague-Dawley rats. In this model system high glucose induced expression of HIF-α and VEGF in a CaMKII-CREB-dependent manner. Activation of this pathway was suggested to be the underlying pathogenesis of retinopathy (38; 39). The newly obtained list of diabetes-induced and CaMKII-dependent retinal genes will be helpful to further study this issue. Conditional deletion of CaMKIIδ in retina vs other glucose storage tissue are also warranted. Our qPCR data demonstrating relatively high expression of all four CaMKII isoforms in retinal tissue in a CaMKIIδ-dependent manner also point to a specific role of CaMKII in the retina, although the induction of the α, β and γ CaMKII isoform can be secondarily triggered by hyperglycemia. Further promoter analysis of these CaMKII genes may lead to a better understanding of this interesting finding.

Putting our observation in a clinical context we can conclude that monitoring glucose and HbA1c levels is not sufficient to predict late complications in diabetic patients, in particular diabetic nephropathy. This is supported by a 10-year follow up study on T2D patients receiving either conventional therapy with dietary restriction or an intensive therapy with either sulfonylurea or insulin or metformin for glucose control (40). The investigators reported that levels of HbA1c in both conventional and intensive treated patients were reduced to the same degree after a one year therapy, and reduction in vascular risk and death from any cause was continued. However, patients receiving an intensified therapy show lesser late complications compared to

patients with simple dietary restriction despite equally adjusted blood glucose. Moreover, it was suggested that normalising blood glucose is not sufficient to prevent diabetic late complications until the acquired metabolic alterations are restored (41). However, to date therapeutic approaches that target reactive metabolites are not shown to combat neither diabetic nephropathy nor retinopathy (42; 43). Based on these observations, recent therapeutic approaches focus on the identification of protective factors that potentially neutralize hyperglycemia-associated damage rather than assessing risk factors. Individuals monitored in the Joslin Medalist Study suffered from long-term T1D (>50years) without presenting the typical late complications and their glycemic control did not correlate with damage neither in kidney nor in retinae (44; 45). Only 12% of the observed diabetic patients suffered from diabetic nephropathy. Individuals with or without diabetic nephropathy from the same study underwent proteomic analysis of glomeruli isolated post-mortem to identify potential protective targets (46). They observed a strongly clustered proteomic signature of enzymes related to glycolysis, the sorbitol pathway, MG production and mitochondrial function suggesting that reduction of free glucose and its reactive metabolites can preserve the kidney function.

Thus, there is an urgent need for innovative treatment strategies to combat diabetic late complications. Our present work suggests that adjusting blood glucose levels in clinical management alone is not sufficient to prevent diabetic patients from organ damage. It is rather necessary to gain a mechanistic understanding leading to failure of individual organ systems in diabetic patients.

Acknowledgments

We thank Jutta Krebs-Haupenthal, Sabine Kuss, Michaela Oestringer and Silvia Harrack for technical help. Furthermore we would like to thank the Center for Model System and Comparative Pathology (Institute of Pathology, University Hospital Heidelberg, Heidelberg, Germany) technical support.

J.C., M.H., J.B., J.M., T.F., H.J.G., H-P.H. and P.P.N. were supported by the SFB 1118, project number 236360313 (Deutsche Forschungsgemeinschaft, DFG). J.C. received the Otto-Hess-scholarship from the German Society for Cardiology. J.B. and H.A.K. were supported by the DZHK (Deutsches Zentrum für Herz-Kreislauf-Forschung - German Centre for Cardiovascular Research) and by the BMBF (German Ministry of Education and Research).

Duality of Interest

There are no potential conflicts of interest relevant to this article.

Author Contributions

J.C., M.H. and J.B. designed the study. J.C., T.F., S.K., M.D., K.H., A.S., M.K., M.P.W., B.P., F.S., J.L., J.M. and A.E. performed experiments. J.C., D.K., P.S., H.-J.G., H.-P.H., C.S., B.B., M.H. and J.B analysed and interpreted the data. H.A.K., H.-J.G., H.-P.H., P.P.N., B.I. and B.B provided research support and conceptual advice. J.C., M.H. and J.B. wrote the paper.

Prior Presentation

Parts of this study were presented in abstract form at the 84th annual meeting of the Deutsche Gesellschaft für Kardiologie (DGK) in April 2018 in Mannheim, Germany

Data and Resource Availability

The datasets generated during and/or analyzed during the current study are available from the corresponding author upon reasonable request.

Guarantor statement

J.B. is the guarantor of this work and, as such, had full access to all the data in the study and takes responsibility for the integrity of the data and the accuracy of the data analysis.

Figure legends

Figure 1

CaMKIIδ-deficient Lepr$^{db/db}$ mice are hyperinsulinemic but not hyperglycemic. **(A)** Time course showing blood glucose levels over a period of 32 weeks in Lepr$^{+/+}$ and Lepr$^{db/db}$ mice with or without CaMKIIδ deficiency. Concentration of blood glucose in Lepr$^{db/db}$/KO mice is reduced to normoglycaemic levels from 24 weeks of age. **(B)** Graph showing levels of blood glucose in animals at 24 weeks of age. **(C)** Levels of HbA1c are increased in Lepr$^{db/db}$/WT and blunted in Lepr$^{db/db}$/KO mice. **(D)** Plasma insulin levels are increased to an equal level in both Lepr$^{db/db}$ groups. Numbers of animals investigated are n≥7 in box and whisker plots or indicated as dots in each group. Values are expressed as mean and SD in scatter plots and as mean and min to max in box and whisker plots. *p<0.05 Lepr$^{db/db}$ vs. Lepr$^{+/+}$, $^{\#}$p<0.05 Lepr$^{db/db}$ vs. Lepr$^{db/db}$/KO, ****p<0.0001, ns=not significant.

Figure 2

CaMKIIδ deficiency improves insulin responsiveness.

(A) Intraperitoneal Glucose tolerance test (GTT) in 13-14 week old animals. Area under the curve analysis (AUC) shows impaired blood glucose normalisation in Lepr$^{db/db}$ groups after intraperitoneal injection of glucose. **(B)** Intraperitoneal insulin tolerance test (ITT) in same animals. AUC analysis indicates improved insulin sensing in Lepr$^{db/db}$ animals. Numbers of animals investigated are indicated as dots. All values are expressed as mean and SD. *p <0.05, ns=not significant.

Figure 3

Evidence for increased glucose transport into skeletal muscle and for downregulated hepatic glucose production in CaMKIIδ-deficient Lepr$^{db/db}$ mice.

(A) Immunoblot showing levels of GLUT1 and GLUT4 in the skeletal muscle of indicated mice, **(B)** graphs showing quantification of immunoblot respectively, β-tubulin was used as loading control. **(C)** Left graph showing increased glycogen levels in skeletal muscle of both Lepr$^{db/db}$/WT and Lepr$^{db/db}$/KO groups compared to their non-diabetic littermates. Right graph shows increased delta of glycogen content in Lepr$^{db/db}$/KO mice compared to their Lepr$^{db/db}$/WT littermates. Numbers of animals

investigated are n=3 in each group or depicted as dots. All values are expressed as mean and SD. *p <0.05, **p <0.01, ***p <0.001, ns=not significant.

Figure 4

Diabetic nephropathy despite normoglycemia in CaMKIIδ-deficient Lepr$^{db/db}$ mice. (A) Representative PAS staining of tissue slides showing glomeruli of indicated animals. PAS positive areas are more prominent in Lepr$^{db/db}$ animals independently from the genotype. **(B)** Electron microscopic images and quantification showing thickening of the basal membrane in both Lepr$^{db/db}$/WT and Lepr$^{db/db}$/KO mice**. (C)** WT-1 staining and quantification showing podocyte loss in both Lepr$^{db/db}$ groups. **(D)** Masson-trichrome staining depicturing equal tubularinterstitial fibrosis in both Lepr$^{db/db}$ groups. **(E)** Graph showing increased Albumin/Creatinine Ratio in both Lepr$^{db/db}$/WT and Lepr$^{db/db}$/KO mice. **(F)** Immunoblot and quantification showing levels of Calcineurin and phospho-Calcineurin in kidneys. Numbers of animals investigated for each group are indicated as dots or n>7 in box and whisker blots. Values are expressed as mean and SD in scatter plots and as mean and min to max in box and whisker plots. *p <0.05, **p<0.01, ns=not significant.

Figure 5

Evidence for increased renal glucose uptake in normoglycemic CaMKIIδ-deficient Lepr$^{db/db}$ mice. (A) Immunoblot and quantification of GLUT1 and GLUT4 in renal tissue of indicated mice. **(B)** Immunoblot and quantification of protein O-GlcNAcylation in renal tissue, graph indicates increased O-GlcNAcylation in Lepr$^{db/db}$/WT and KO mice with or without Lepr$^{db/db}$ background. **(C)** Levels of Methylglyoxal (MG) are increased in both WT and KO Lepr$^{db/db}$ mice. Numbers of animals investigated for each group are indicated as dots. All values are expressed as mean and SD. *p <0.05, **p<0.01, ***p <0.001, ****p<0.0001, ns=not significant.

Figure 6

No diabetic retinopathy in normoglycemic CaMKIIδ-deficient Lepr$^{db/db}$ mice. **(A)** Representative retinae tissue slides taken from Lepr$^{+/+}$ and Lepr$^{db/db}$ mice with or without knockout of CaMKIIδ. Blue arrow shows a migrating pericyte, green arrow shows acellular capillaries. **(B)** Numbers of acellular capillaries are increased in Lepr$^{db/db}$/WT animals and at levels of Lepr$^{+/+}$/WT mice in Lepr$^{db/db}$/KO mice. **(C)**

Graph shows loss of pericytes in $Lepr^{db/db}$/WT mice compared to their $Lepr^{+/+}$ littermates. Number of pericytes in $Lepr^{db/db}$/KO mice remained unchanged. **(D)** Graph indicates elevated numbers of migrating pericytes in $Lepr^{db/db}$/WT animals. Numbers of migrating cells is blunted in $Lepr^{db/db}$/KO animals. **(E)** Venn Diagram of significantly regulated genes in retinae and kidneys in WT or KO ($Lepr^{db/db}$ vs. $Lepr^{+/+}$). Dark-blue coloured field represents significantly regulated genes only in retinas of WT but not of KO mice ("594 counts"). Light-blue field represents significantly regulated genes in retina of WT mice and in kidneys of WT mice but not retinas of KO mice ("174 counts"). **(F)** Heatmap of genes regulated in WT retina under diabetic conditions but not in KO. Genes only regulated in the retina are marked in red. Numbers of animals investigated are indicated as dots (B-D) or n≥3 in each group (E-F). All values are expressed as mean and SD. ***p<0.001, ****p<0.0001, ns=not significant.

Figure 7

Working model

CaMKIIδ is required for the development of hyperglycemia in type 2 diabetes (T2D). Diabetic retinopathy but not nephropathy depends on CaMKIIδ.

References

1. Organization WH: Global Report on Diabetes. 2016;
2. Diabetes C, Complications Trial Research G, Nathan DM, Genuth S, Lachin J, Cleary P, Crofford O, Davis M, Rand L, Siebert C: The effect of intensive treatment of diabetes on the development and progression of long-term complications in insulin-dependent diabetes mellitus. N Engl J Med 1993;329:977-986
3. Lachin JM, Genuth S, Nathan DM, Zinman B, Rutledge BN: Effect of glycemic exposure on the risk of microvascular complications in the diabetes control and complications trial--revisited. Diabetes 2008;57:995-1001
4. Luo M, Guan X, Luczak ED, Lang D, Kutschke W, Gao Z, Yang J, Glynn P, Sossalla S, Swaminathan PD, Weiss RM, Yang B, Rokita AG, Maier LS, Efimov IR, Hund TJ, Anderson ME: Diabetes increases mortality after myocardial infarction by oxidizing CaMKII. J Clin Invest 2013;123:1262-1274
5. Braun AP, Schulman H: The multifunctional calcium/calmodulin-dependent protein kinase: from form to function. Annual review of physiology 1995;57:417-445
6. Erickson JR, Joiner ML, Guan X, Kutschke W, Yang J, Oddis CV, Bartlett RK, Lowe JS, O'Donnell SE, Aykin-Burns N, Zimmerman MC, Zimmerman K, Ham AJ, Weiss RM, Spitz DR, Shea MA, Colbran RJ, Mohler PJ, Anderson ME: A dynamic pathway for calcium-independent activation of CaMKII by methionine oxidation. Cell 2008;133:462-474
7. Erickson JR, Pereira L, Wang L, Han G, Ferguson A, Dao K, Copeland RJ, Despa F, Hart GW, Ripplinger CM, Bers DM: Diabetic hyperglycaemia activates CaMKII and arrhythmias by O-linked glycosylation. Nature 2013;502:372-376
8. Kronlage M, Dewenter M, Grosso J, Fleming T, Oehl U, Lehmann LH, Falcao-Pires I, Leite-Moreira AF, Volk N, Grone HJ, Muller OJ, Sickmann A, Katus HA, Backs J: O-GlcNAcylation of Histone Deacetylase 4 Protects the Diabetic Heart From Failure. Circulation 2019;140:580-594
9. Ozcan L, Wong CC, Li G, Xu T, Pajvani U, Park SK, Wronska A, Chen BX, Marks AR, Fukamizu A, Backs J, Singer HA, Yates JR, 3rd, Accili D, Tabas I: Calcium signaling through CaMKII regulates hepatic glucose production in fasting and obesity. Cell Metab 2012;15:739-751
10. Ozcan L, Cristina de Souza J, Harari AA, Backs J, Olson EN, Tabas I: Activation of calcium/calmodulin-dependent protein kinase II in obesity mediates suppression of hepatic insulin signaling. Cell Metab 2013;18:803-815
11. Ozcan L, Ghorpade DS, Zheng Z, de Souza JC, Chen K, Bessler M, Bagloo M, Schrope B, Pestell R, Tabas I: Hepatocyte DACH1 Is Increased in Obesity via Nuclear Exclusion of HDAC4 and Promotes Hepatic Insulin Resistance. Cell Rep 2016;15:2214-2225
12. Backs J, Backs T, Neef S, Kreusser MM, Lehmann LH, Patrick DM, Grueter CE, Qi X, Richardson JA, Hill JA, Katus HA, Bassel-Duby R, Maier LS, Olson EN: The delta isoform of CaM kinase II is required for pathological cardiac hypertrophy and remodeling after pressure overload. Proc Natl Acad Sci U S A 2009;106:2342-2347
13. Dietrich N, Hammes HP: Retinal digest preparation: a method to study diabetic retinopathy. Methods Mol Biol 2012;933:291-302
14. Hirose K, Osterby R, Nozawa M, Gundersen HJ: Development of glomerular lesions in experimental long-term diabetes in the rat. Kidney international 1982;21:689-695

15. Madhusudhan T, Ghosh S, Wang H, Dong W, Gupta D, Elwakiel A, Stoyanov S, Al-Dabet MdM, Krishnan S, Biemann R, Nazir S, Zimmermann S, Mathew A, Gadi I, Rana R, Zeng-Brouwers J, Moeller MJ, Schaefer L, Esmon CT, Kohli S, Reiser J, Rezaie AR, Ruf W, Isermann B: Podocyte Integrin-β₃ and Activated Protein C Coordinately Restrict RhoA Signaling and Ameliorate Diabetic Nephropathy. Journal of the American Society of Nephrology 2020;31:1762-1780
16. Livak KJ, Schmittgen TD: Analysis of relative gene expression data using real-time quantitative PCR and the 2(-Delta Delta C(T)) Method. Methods 2001;25:402-408
17. Rabbani N, Thornalley PJ: Measurement of methylglyoxal by stable isotopic dilution analysis LC-MS/MS with corroborative prediction in physiological samples. Nat Protoc 2014;9:1969-1979
18. Backman TWH, Girke T: systemPipeR: NGS workflow and report generation environment. BMC Bioinformatics 2016;17:388
19. Bray NL, Pimentel H, Melsted P, Pachter L: Near-optimal probabilistic RNA-seq quantification. Nature Biotechnology 2016;34:525-527
20. Ritchie ME, Phipson B, Wu D, Hu Y, Law CW, Shi W, Smyth GK: limma powers differential expression analyses for RNA-sequencing and microarray studies. Nucleic Acids Res 2015;43:e47
21. Gu Z, Eils R, Schlesner M: Complex heatmaps reveal patterns and correlations in multidimensional genomic data. Bioinformatics 2016;32:2847-2849
22. Sergushichev AA: An algorithm for fast preranked gene set enrichment analysis using cumulative statistic calculation. bioRxiv 2016:060012
23. Geistlinger L, Csaba G, Zimmer R: Bioconductor's EnrichmentBrowser: seamless navigation through combined results of set- & network-based enrichment analysis. BMC Bioinformatics 2016;17:45
24. Bligh EG, Dyer WJ: A rapid method of total lipid extraction and purification. Can J Biochem Physiol 1959;37:911-917
25. Mucksch F, Citir M, Luchtenborg C, Glass B, Traynor-Kaplan A, Schultz C, Brugger B, Krausslich HG: Quantification of phosphoinositides reveals strong enrichment of PIP2 in HIV-1 compared to producer cell membranes. Sci Rep 2019;9:17661
26. Ozbalci C, Sachsenheimer T, Brugger B: Quantitative analysis of cellular lipids by nano-electrospray ionization mass spectrometry. Methods Mol Biol 2013;1033:3-20
27. Gould GW, Holman GD: The glucose transporter family: structure, function and tissue-specific expression. Biochem J 1993;295 (Pt 2):329-341
28. Cao W, Collins QF, Becker TC, Robidoux J, Lupo EG, Jr., Xiong Y, Daniel KW, Floering L, Collins S: p38 Mitogen-activated protein kinase plays a stimulatory role in hepatic gluconeogenesis. J Biol Chem 2005;280:42731-42737
29. Kreusser MM, Lehmann LH, Keranov S, Hoting MO, Oehl U, Kohlhaas M, Reil JC, Neumann K, Schneider MD, Hill JA, Dobrev D, Maack C, Maier LS, Grone HJ, Katus HA, Olson EN, Backs J: Cardiac CaM Kinase II genes delta and gamma contribute to adverse remodeling but redundantly inhibit calcineurin-induced myocardial hypertrophy. Circulation 2014;130:1262-1273
30. Fulop N, Marchase RB, Chatham JC: Role of protein O-linked N-acetyl-glucosamine in mediating cell function and survival in the cardiovascular system. Cardiovascular research 2007;73:288-297
31. Thornalley PJ: The glyoxalase system: new developments towards functional characterization of a metabolic pathway fundamental to biological life. Biochem J 1990;269:1-11

32. Hammes HP, Lin J, Renner O, Shani M, Lundqvist A, Betsholtz C, Brownlee M, Deutsch U: Pericytes and the pathogenesis of diabetic retinopathy. Diabetes 2002;51:3107-3112
33. Illario M, Monaco S, Cavallo AL, Esposito I, Formisano P, D'Andrea L, Cipolletta E, Trimarco B, Fenzi G, Rossi G, Vitale M: Calcium-calmodulin-dependent kinase II (CaMKII) mediates insulin-stimulated proliferation and glucose uptake. Cell Signal 2009;21:786-792
34. Ojuka EO, Goyaram V, Smith JA: The role of CaMKII in regulating GLUT4 expression in skeletal muscle. Am J Physiol Endocrinol Metab 2012;303:E322-331
35. Backs J, Song K, Bezprozvannaya S, Chang S, Olson EN: CaM kinase II selectively signals to histone deacetylase 4 during cardiomyocyte hypertrophy. J Clin Invest 2006;116:1853-1864
36. Ozcan L, Xu X, Deng SX, Ghorpade DS, Thomas T, Cremers S, Hubbard B, Serrano-Wu MH, Gaestel M, Landry DW, Tabas I: Treatment of Obese Insulin-Resistant Mice With an Allosteric MAPKAPK2/3 Inhibitor Lowers Blood Glucose and Improves Insulin Sensitivity. Diabetes 2015;64:3396-3405
37. Sas KM, Kayampilly P, Byun J, Nair V, Hinder LM, Hur J, Zhang H, Lin C, Qi NR, Michailidis G, Groop PH, Nelson RG, Darshi M, Sharma K, Schelling JR, Sedor JR, Pop-Busui R, Weinberg JM, Soleimanpour SA, Abcouwer SF, Gardner TW, Burant CF, Feldman EL, Kretzler M, Brosius FC, 3rd, Pennathur S: Tissue-specific metabolic reprogramming drives nutrient flux in diabetic complications. JCI Insight 2016;1:e86976
38. Li J, Wang P, Yu S, Zheng Z, Xu X: Calcium entry mediates hyperglycemia-induced apoptosis through Ca(2+)/calmodulin-dependent kinase II in retinal capillary endothelial cells. Mol Vis 2012;18:2371-2379
39. Li J, Zhao SZ, Wang PP, Yu SP, Zheng Z, Xu X: Calcium mediates high glucose-induced HIF-1alpha and VEGF expression in cultured rat retinal Muller cells through CaMKII-CREB pathway. Acta pharmacologica Sinica 2012;33:1030-1036
40. Holman RR, Paul SK, Bethel MA, Matthews DR, Neil HA: 10-year follow-up of intensive glucose control in type 2 diabetes. N Engl J Med 2008;359:1577-1589
41. Fleming T, Cuny J, Nawroth G, Djuric Z, Humpert PM, Zeier M, Bierhaus A, Nawroth PP: Is diabetes an acquired disorder of reactive glucose metabolites and their intermediates? Diabetologia 2012;55:1151-1155
42. The effect of ruboxistaurin on visual loss in patients with moderately severe to very severe nonproliferative diabetic retinopathy: initial results of the Protein Kinase C beta Inhibitor Diabetic Retinopathy Study (PKC-DRS) multicenter randomized clinical trial. Diabetes 2005;54:2188-2197
43. Bolton WK, Cattran DC, Williams ME, Adler SG, Appel GB, Cartwright K, Foiles PG, Freedman BI, Raskin P, Ratner RE, Spinowitz BS, Whittier FC, Wuerth JP: Randomized trial of an inhibitor of formation of advanced glycation end products in diabetic nephropathy. American journal of nephrology 2004;24:32-40
44. Sun JK, Keenan HA, Cavallerano JD, Asztalos BF, Schaefer EJ, Sell DR, Strauch CM, Monnier VM, Doria A, Aiello LP, King GL: Protection from retinopathy and other complications in patients with type 1 diabetes of extreme duration: the joslin 50-year medalist study. Diabetes Care 2011;34:968-974
45. Keenan HA, Costacou T, Sun JK, Doria A, Cavellerano J, Coney J, Orchard TJ, Aiello LP, King GL: Clinical factors associated with resistance to microvascular complications in diabetic patients of extreme disease duration: the 50-year medalist study. Diabetes Care 2007;30:1995-1997
46. Qi W, Keenan HA, Li Q, Ishikado A, Kannt A, Sadowski T, Yorek MA, Wu IH, Lockhart S, Coppey LJ, Pfenninger A, Liew CW, Qiang G, Burkart AM, Hastings S,

Pober D, Cahill C, Niewczas MA, Israelsen WJ, Tinsley L, Stillman IE, Amenta PS, Feener EP, Vander Heiden MG, Stanton RC, King GL: Pyruvate kinase M2 activation may protect against the progression of diabetic glomerular pathology and mitochondrial dysfunction. Nat Med 2017;23:753-762

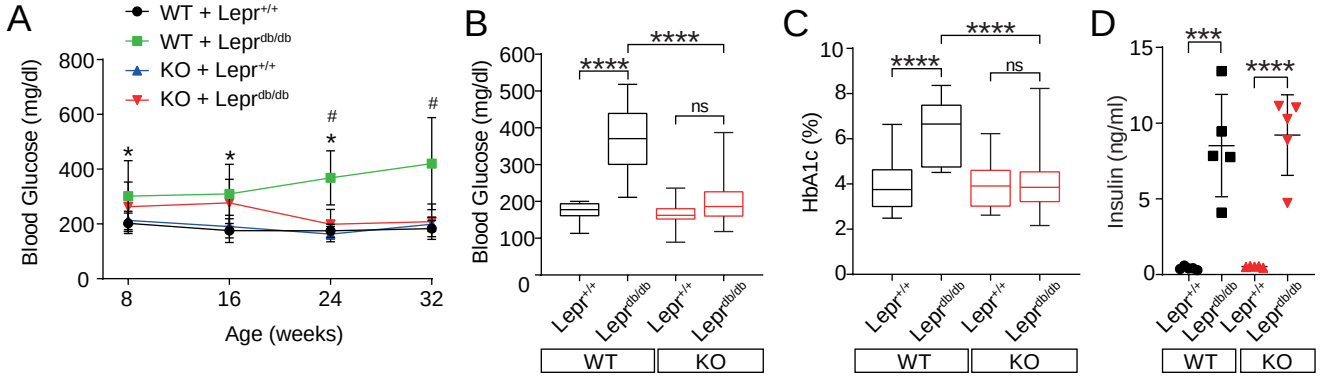
A
WT + Lepr+/+
WT + Leprdb/db
KO + Lepr+/+
KO + Leprdb/db
Blood Glucose (mg/dl)
Age (weeks)
B
Blood Glucose (mg/dl)
****
****
ns
C
HbA1c (%)
****
****
ns
D
Insulin (ng/ml)
***
****
Lepr+/+
Leprdb/db
WT
KO

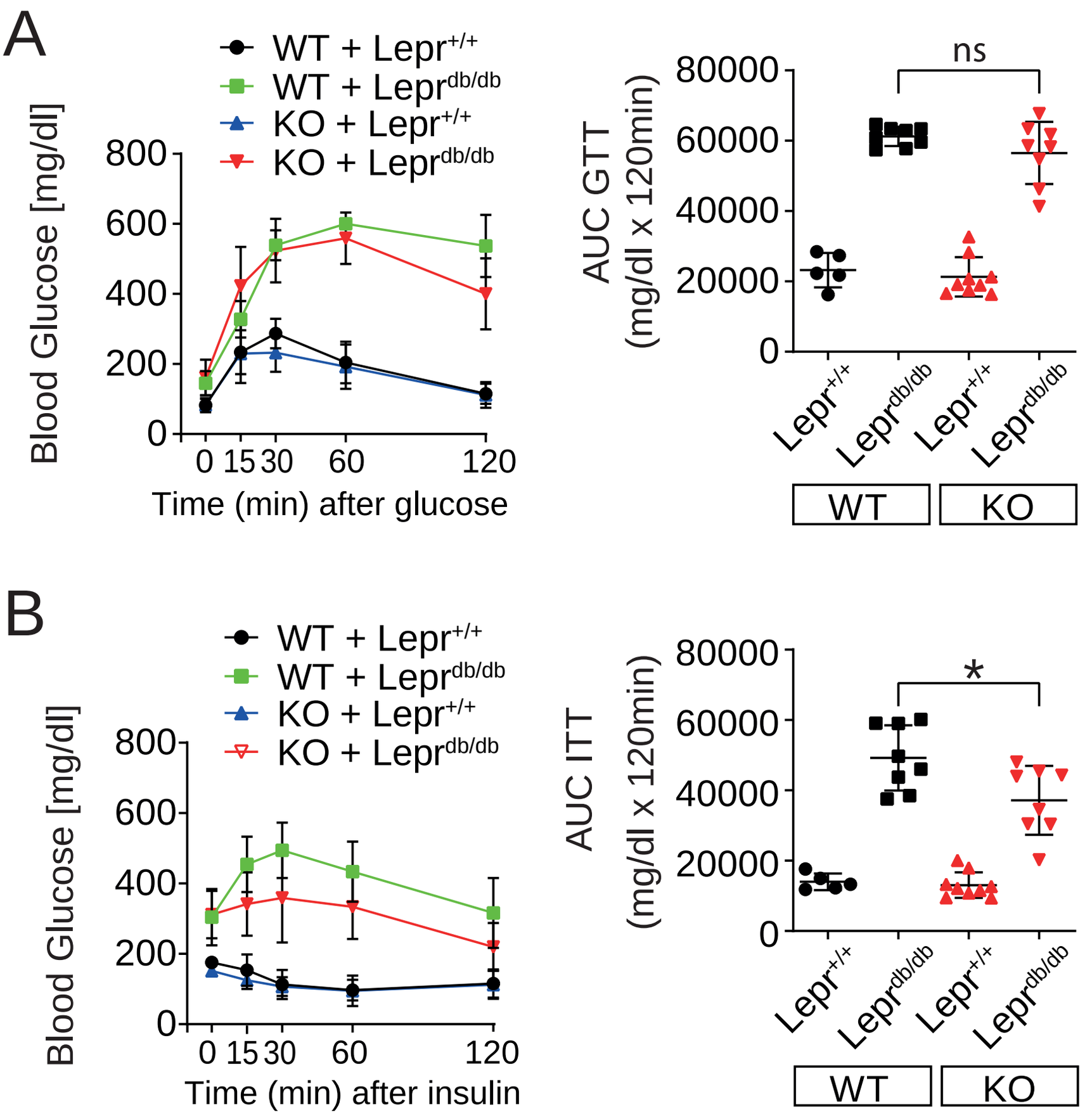
A
WT + Lepr+/+
WT + Leprdb/db
KO + Lepr+/+
KO + Leprdb/db
Blood Glucose [mg/dl]
800
600
400
200
0
0 15 30 60 120
Time (min) after glucose
ns
AUC GTT
(mg/dl x 120min)
80000
60000
40000
20000
0
Lepr+/+
Leprdb/db
Lepr+/+
Leprdb/db
WT
KO
B
WT + Lepr+/+
WT + Leprdb/db
KO + Lepr+/+
KO + Leprdb/db
Blood Glucose [mg/dl]
800
600
400
200
0
0 15 30 60 120
Time (min) after insulin
*
AUC ITT
(mg/dl x 120min)
80000
60000
40000
20000
0
Lepr+/+
Leprdb/db
Lepr+/+
Leprdb/db
WT
KO

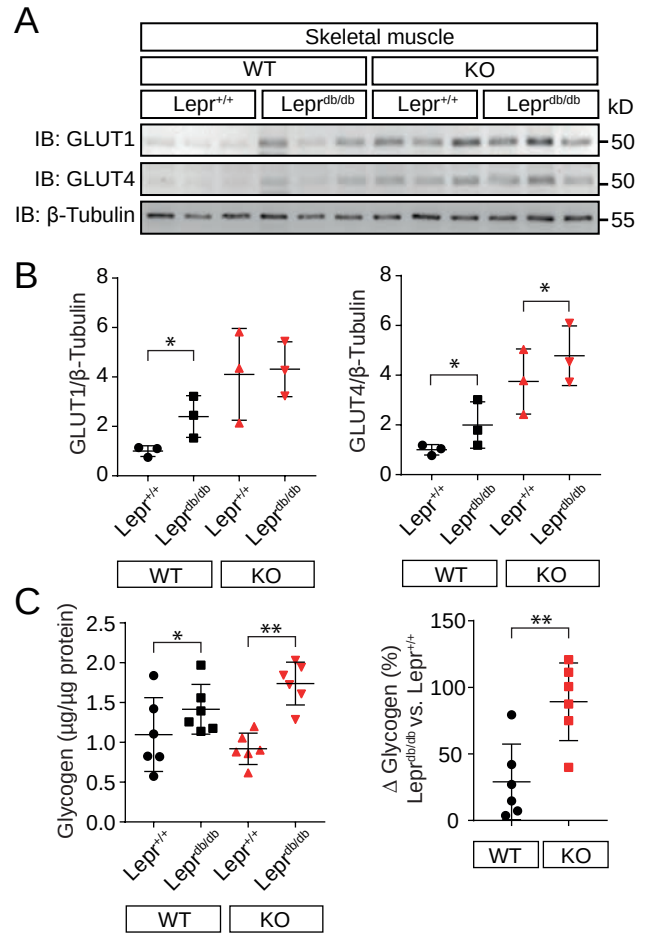
A
Skeletal muscle
WT
KO
Lepr+/+
Leprdb/db
Lepr+/+
Leprdb/db
kD
IB: GLUT1
50
IB: GLUT4
50
IB: β-Tubulin
55
B
GLUT1/β-Tubulin
GLUT4/β-Tubulin
WT
KO
C
Glycogen (μg/μg protein)
Δ Glycogen (%)
Leprdb/db vs. Lepr+/+
WT
KO

Figure 4

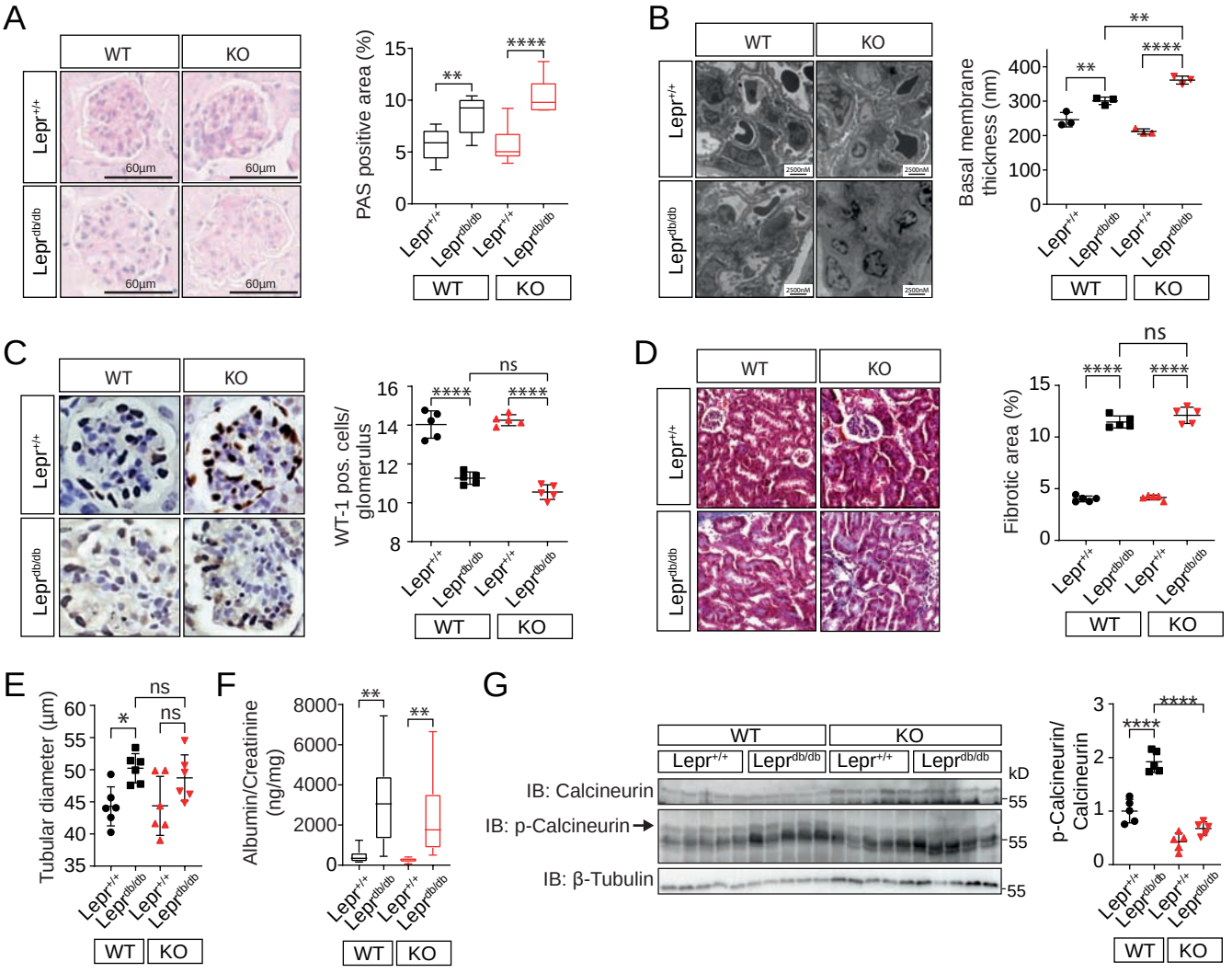
A
WT
KO
Lepr+/+
Leprdb/db
60µm
PAS positive area (%)
B
Basal membrane thickness (nm)
C
WT-1 pos. cells/ glomerulus
D
Fibrotic area (%)
ns
E
Tubular diameter (µm)
F
Albumin/Creatinine (ng/mg)
G
IB: Calcineurin
IB: p-Calcineurin
IB: β-Tubulin
kD
55
p-Calcineurin/ Calcineurin

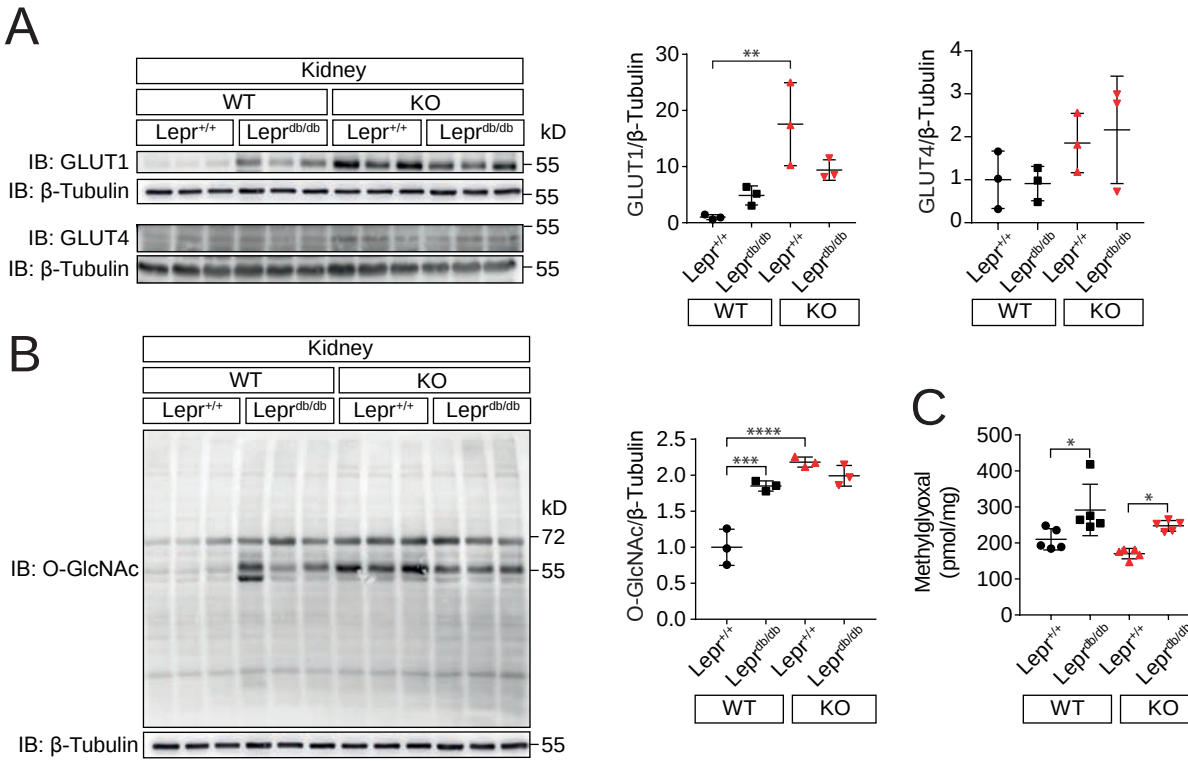
A
Kidney
WT
KO
Lepr+/+
Leprdb/db
Lepr+/+
Leprdb/db
kD
IB: GLUT1
55
IB: β-Tubulin
55
IB: GLUT4
55
IB: β-Tubulin
55
GLUT1/β-Tubulin
30
20
10
0
**
GLUT4/β-Tubulin
4
3
2
1
0
B
Kidney
WT
KO
Lepr+/+
Leprdb/db
Lepr+/+
Leprdb/db
kD
72
IB: O-GlcNAc
55
IB: β-Tubulin
55
O-GlcNAc/β-Tubulin
2.5
2.0
1.5
1.0
0.5
0.0
****
***
C
Methylglyoxal (pmol/mg)
500
400
300
200
100
0
*
*

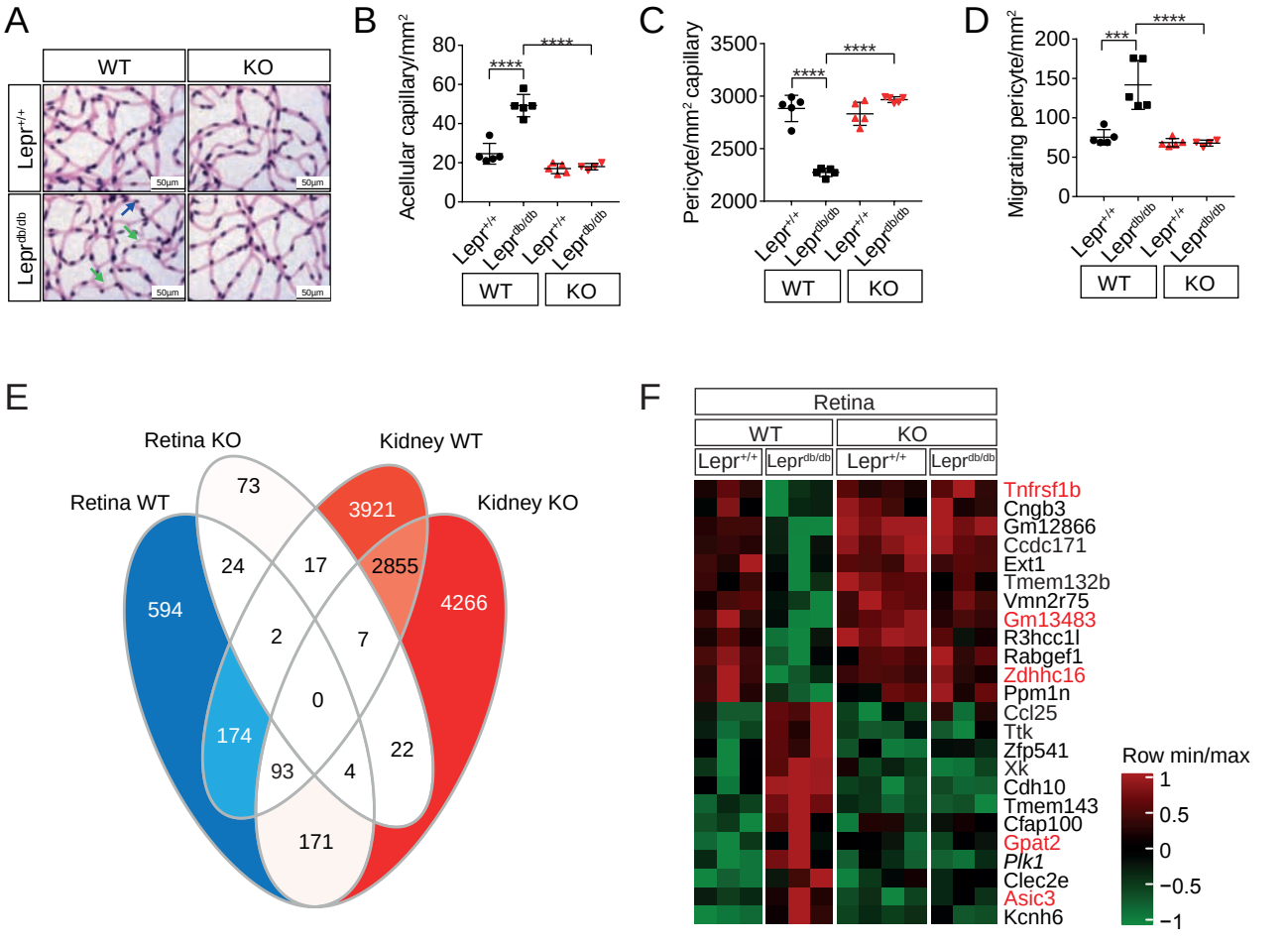
A
WT
KO
Lepr+/+
Leprdb/db
50μm
B
Acellular capillary/mm2
****
****
Lepr+/+
Leprdb/db
Lepr+/+
Leprdb/db
WT
KO
C
Pericyte/mm2 capillary
****
****
D
Migrating pericyte/mm2
***
****
E
Retina KO
Kidney WT
Retina WT
Kidney KO
73
3921
24
17
2855
594
4266
2
7
0
174
22
93
4
171
F
Retina
WT
KO
Lepr+/+
Leprdb/db
Lepr+/+
Leprdb/db
Tnfrsf1b
Cngb3
Gm12866
Ccdc171
Ext1
Tmem132b
Vmn2r75
Gm13483
R3hcc1l
Rabgef1
Zdhhc16
Ppm1n
Ccl25
Ttk
Zfp541
Xk
Cdh10
Tmem143
Cfap100
Gpat2
Plk1
Clec2e
Asic3
Kcnh6
Row min/max
1
0.5
0
−0.5
−1

Figure 7

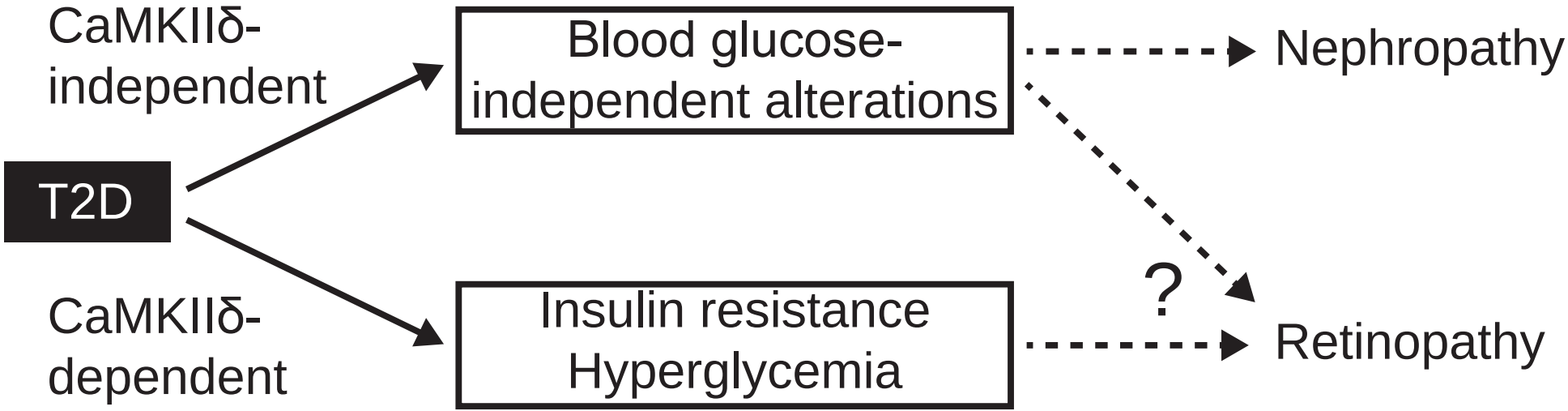
CaMKIIδ-independent
Blood glucose-independent alterations
Nephropathy
T2D
?
CaMKIIδ-dependent
Insulin resistance Hyperglycemia
Retinopathy

Supplementary data

Supplementary Figure S1: (A-C) Box and whisker plots showing bodyweights of $Lepr^{+/+}$ (WT/KO) and $Lepr^{db/db}$ (WT/KO) mice at age of 8, 16 and 24 weeks respectively. Numbers of animals investigated are n≥8. Values are expressed as mean and min to max. ****p <0.0001, ns=not significant.

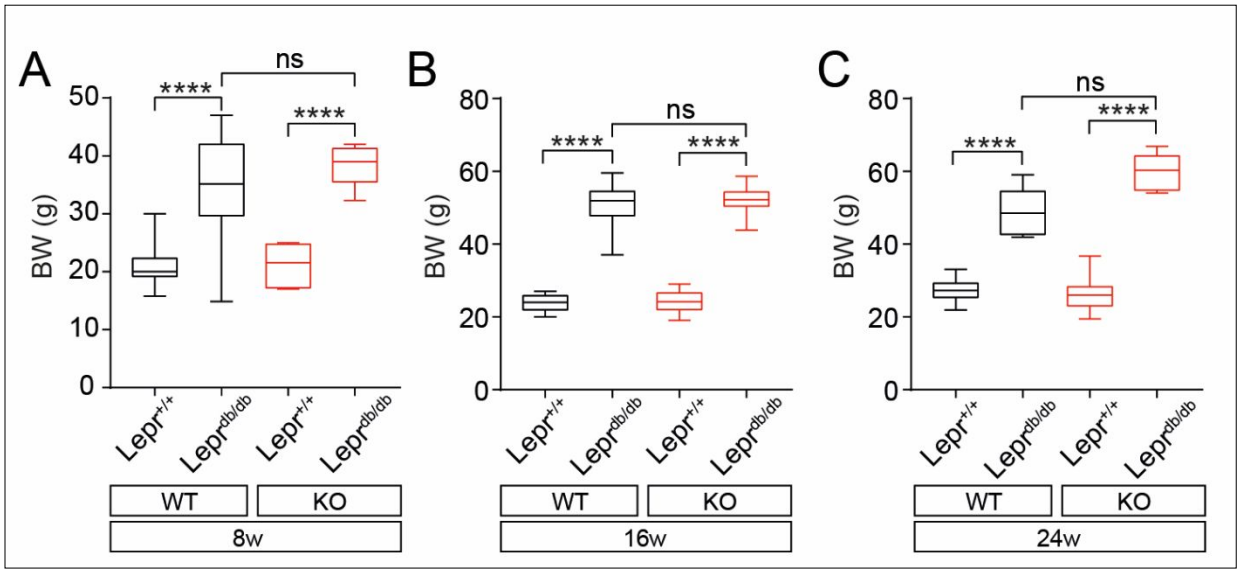

Supplementary Figure S2: Levels of sorbitol in skeletal muscle are equal in $Lepr^{+/+}$ and $Lepr^{db/db}$ conditions in WT and KO animals. Numbers of investigated animals are indicated as dots. All values are expressed as mean and SD.

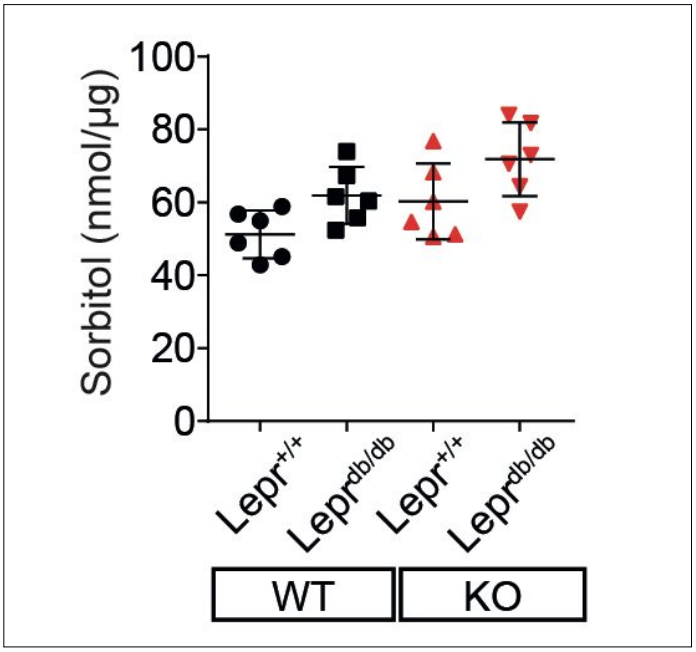

Supplementary Figure S3: (A) Glycogen and **(B)** Sorbitol content in liver tissue of indicated mice. Numbers of investigated animals are indicated as dots. All values are expressed as mean and SD. *p <0.05.

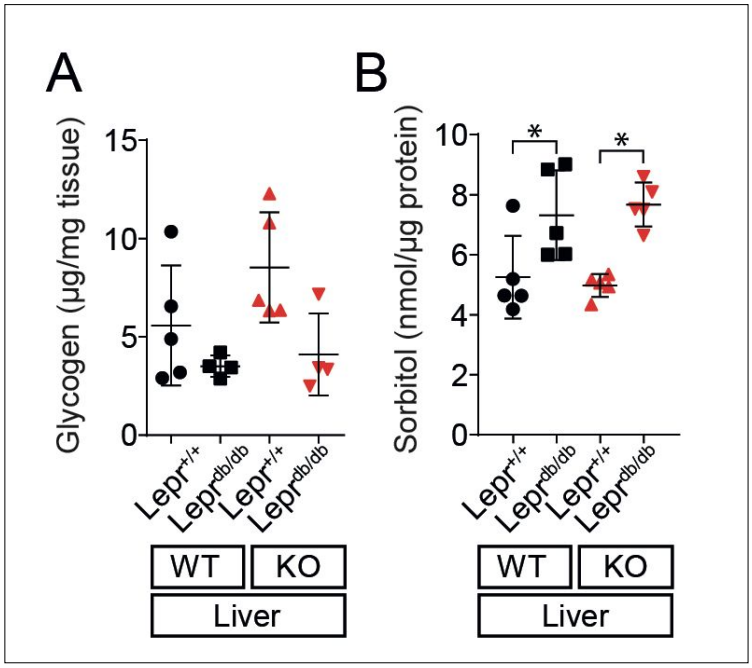

Supplementary Figure S4: (A) Immunoblot showing phosphorylated and total p-38 MAPK levels in livers of indicated mice, β-tubulin was used as loading control. **(B)** Graph showing reduced phosphorylation of p-38 MAPK in Lepr$^{db/db}$/KO animals. mRNA expression of *Pck-1* **(C)** and *G6pc* **(D)** is reduced in Lepr$^{db/db}$/KO compared to Lepr$^{db/db}$/WT mice. **(E)** mRNA expression of CaMKII-α, -β, -γ and -δ isoforms in liver. Numbers of animals investigated are indicated as dots. All values are expressed as mean and SD. *p <0.05, **p<0.01, ****p <0.0001, ns=not significant, n.d.=not detectable.

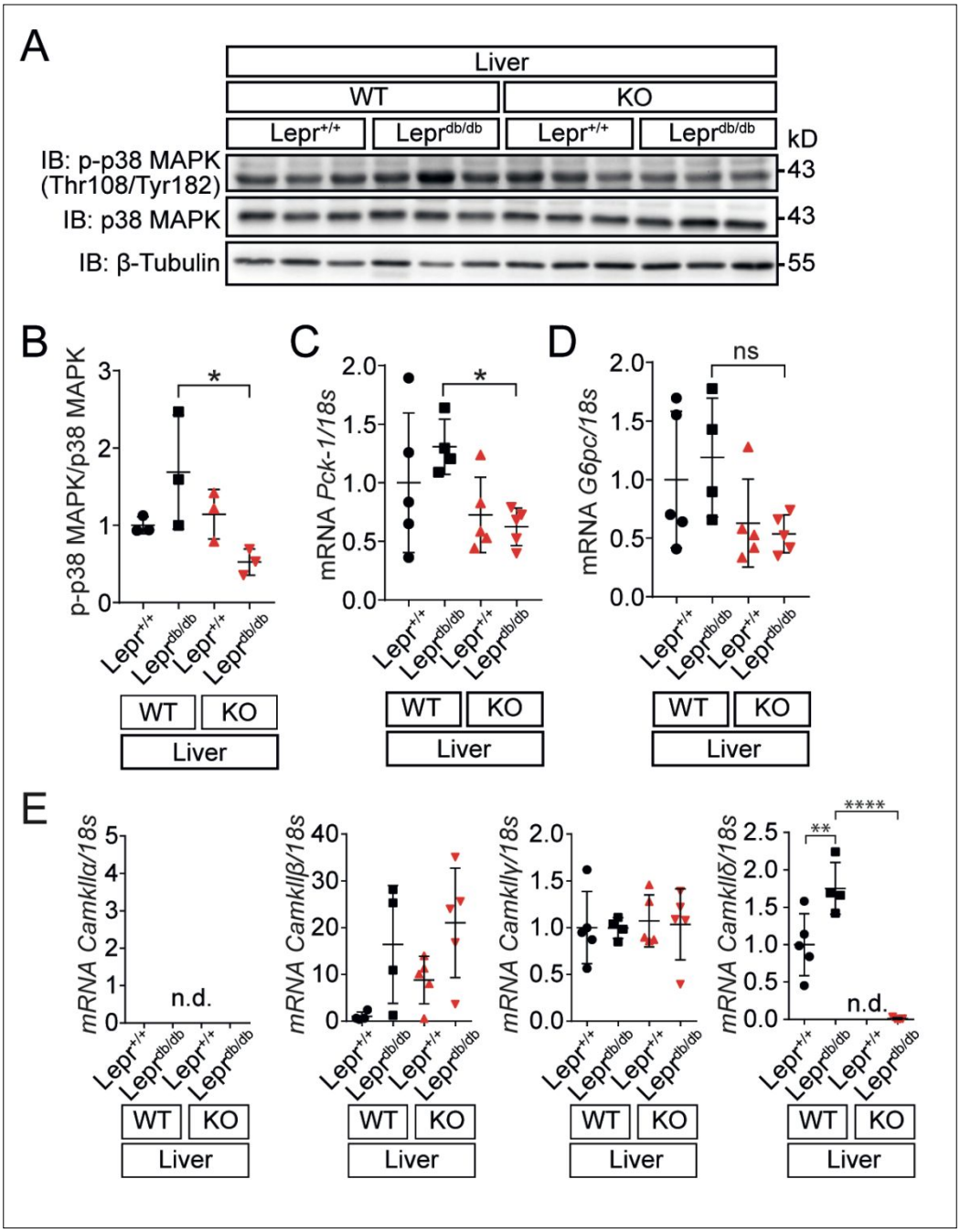

Supplementary Figure S5: (A/B) mRNA expression of renal *Sglt2* and *Sglt1* normalized to 18s mRNA respectively. **(C)** Urinary glucose concentrations of indicated mice normalized to creatinine. Numbers of animals investigated are indicated as dots. All values are expressed as mean and SD. *p <0.05, **p<0.01, ns=not significant.

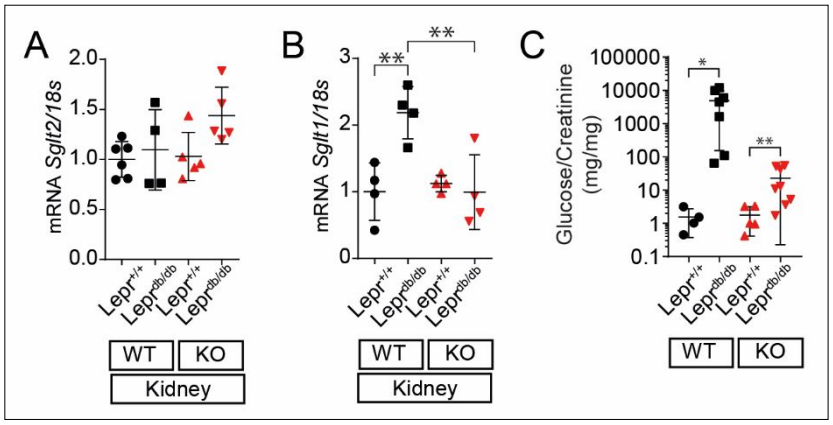

Supplementary Figure S6: (A/B) Kidney weight and relative glomerulum size of 8- and **(C/D)** 16 week old mice showing glomerular hypertrophy in both Lepr$^{db/db}$ (WT and KO) groups. Numbers of animals investigated are indicated as dots or n≥8 in box and whisker plots. Values are expressed as mean and SD in scatter plots and as mean and min to max in box and whisker plots. *p <0.05, *p<0.01, ****p <0.0001, ns=not significant.

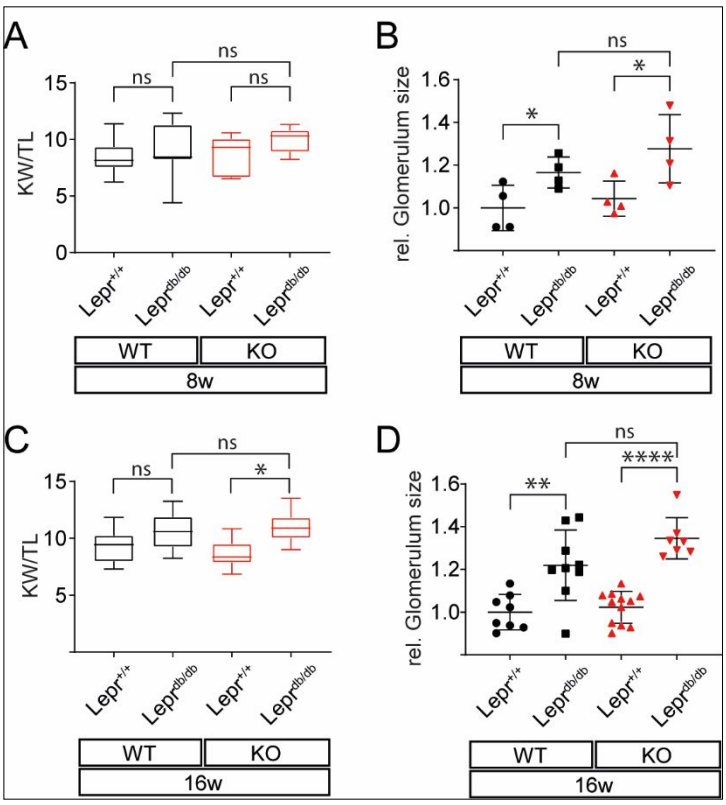

Supplementary Figure S7: (A) mRNA expression of *CaMKII-α, -β, -γ* and *-δ* isoforms in kidney and **(B)** in retina. Numbers of animals investigated are indicated as dots. All values are expressed as mean and SD. *p <0.05, **p<0.01, ****p <0.0001, n.d.=not detectable.

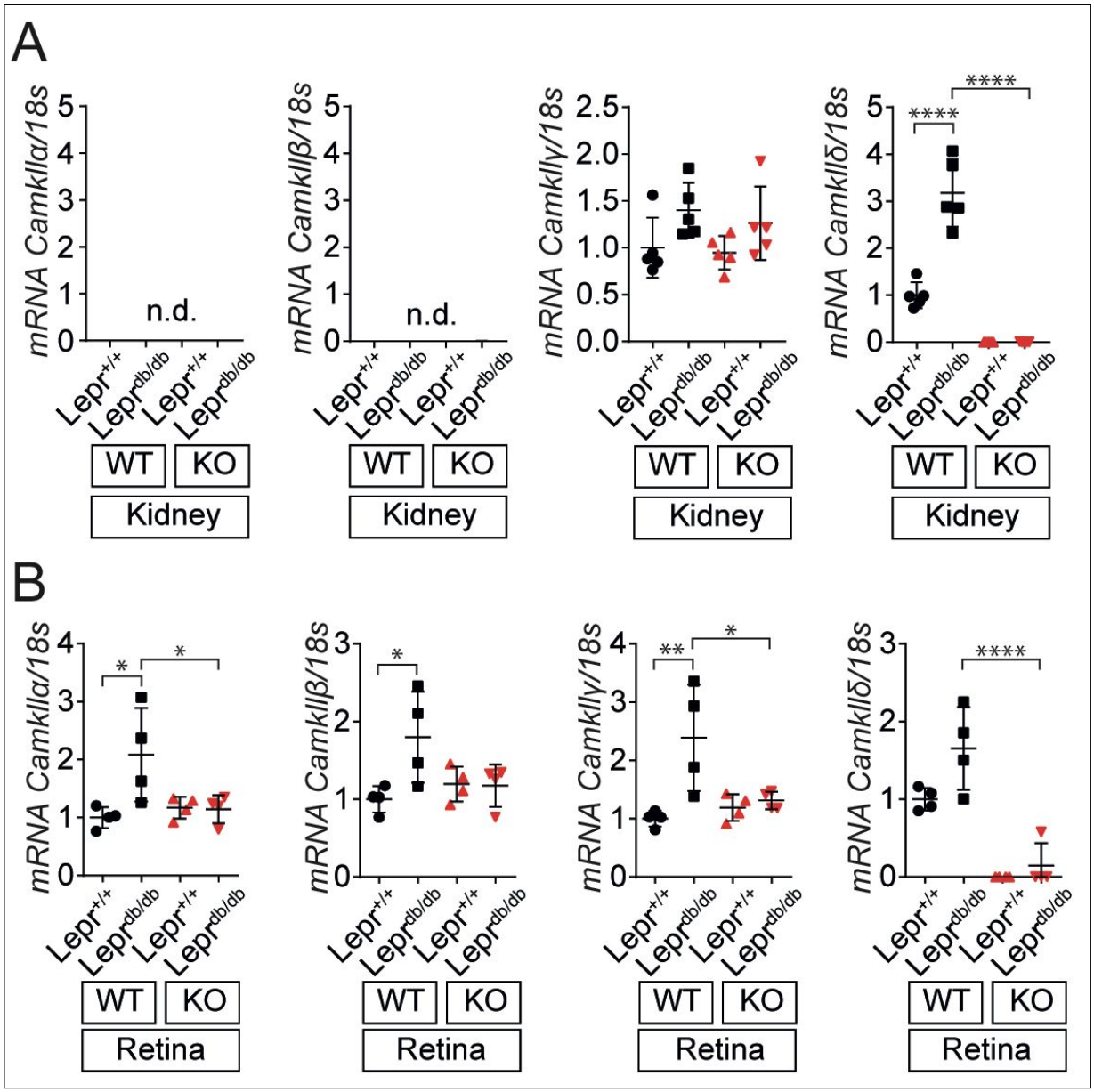

Supplementary Figure S8: (A/C) Immunoblot demonstrating successful siRNA mediated knockdown of CaMKII in M1 and MES13 cells. **(B/D)** Glycolysis stress test performed with a seahorse analyser in M1 and MES13 cells.

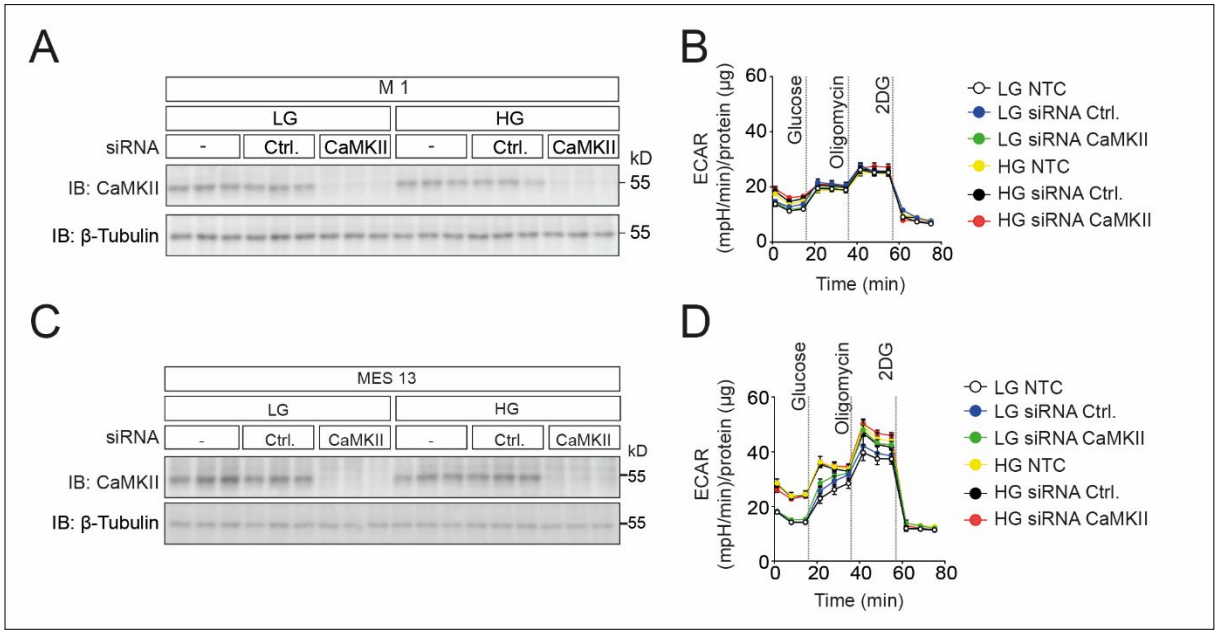

Supplementary Figure S9: (A/B) Heatmaps of top regulated genes in WT kidney *or* WT retina compared to KO in retina or kidney. **(C/D)** Heatmaps of genes differentially regulated in retina *and* kidney of WT mice but not in retina of KO mice. Numbers of animals investigated are n=4 in A and C and n≥3 in B and D.

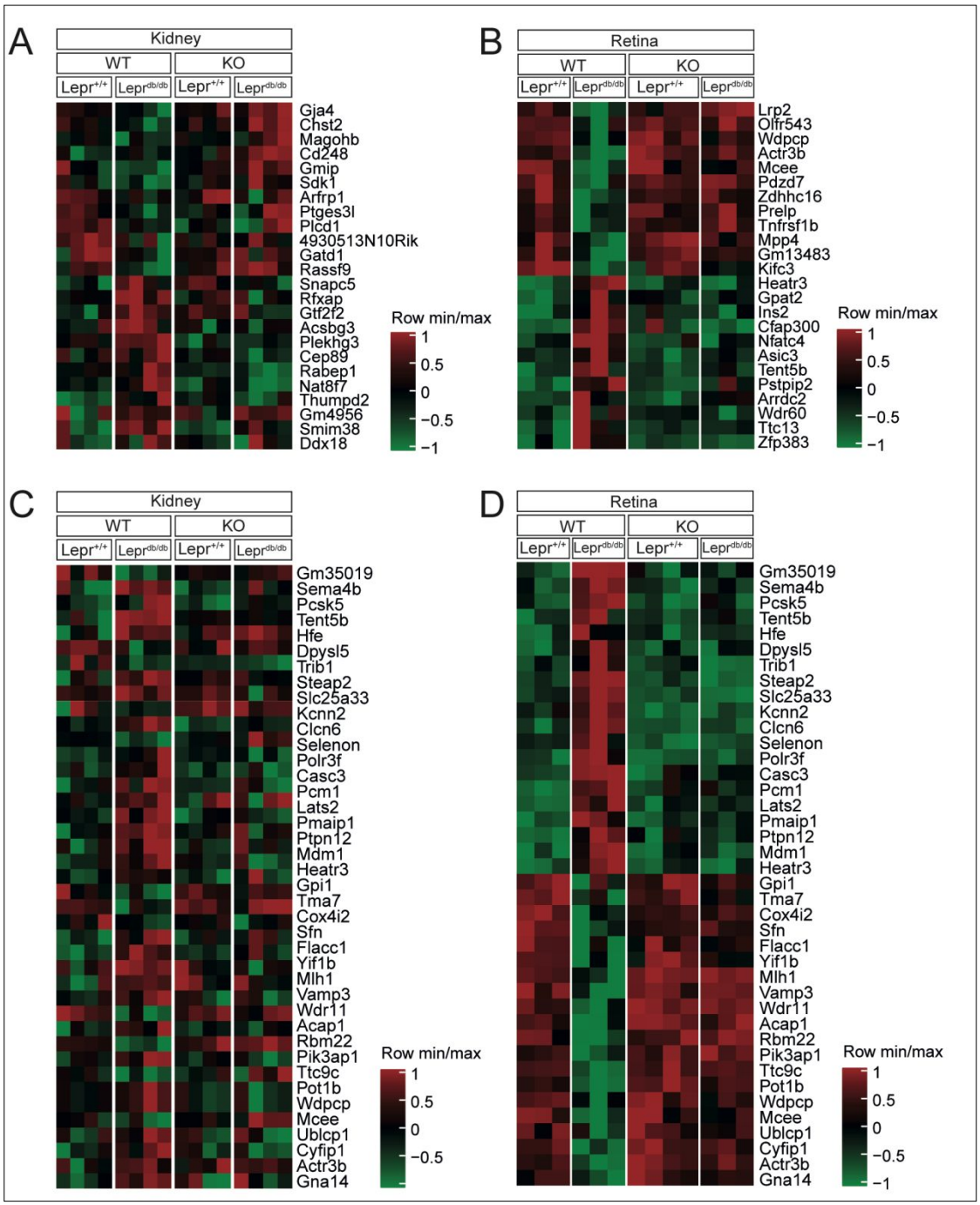

Supplementary Figure S10: (A) Heatmap of differentially regulated genes involved in lipid metabolism in retina and **(B)** kidney. **(C)** Heatmap of lipid classes represents only minor changes of lipidome in serum, kidney and retina between the indicated groups. (D) PCA plots of lipidome changes in serum, kidney and retina Lepr$^{+/+}$/WT vs. Lepr$^{db/db}$/WT (left diagrams) and Lepr$^{+/+}$/KO vs. Lepr$^{db/db}$/KO. **(E)** Bar graph showing levels of Phosphatidyl ethanolamine (PE) and Cholesterol (Chol) in Retina. Numbers of animals investigated are n≥3 in A and B and n≥4 in C-E.